Modeling of particle interactions in magnetorheological elastomers

A. M. Biller,[a] O. V. Stolbov,[b] and Yu. L. Raikher[c]
Institute of Continuous Media Mechanics, Ural Branch of Russian Academy of Sciences, Perm 614013, Russia

(Received 27 July 2014; accepted 5 September 2014; published online 18 September 2014)

The interaction between two particles made of an isotropic linearly polarizable magnetic material and embedded in an elastomer matrix is studied. In this case, when an external field is imposed, the magnetic attraction of the particles, contrary to point dipoles, is almost wraparound. The exact solution of the magnetic problem in the linear polarization case, although existing, is not practical; to circumvent its use, an interpolation formula is proposed. One more interpolation expression is developed for the resistance of the elastic matrix to the field-induced particle displacements. Minimization of the total energy of the pair reveals its configurational bistability in a certain field range. One of the possible equilibrium states corresponds to the particles dwelling at a distance, the other—to their collapse in a tight dimer. This mesoscopic bistability causes magnetomechanical hysteresis which has important implications for the macroscopic behavior of magnetorheological elastomers. © *2014 AIP Publishing LLC*. [http://dx.doi.org/10.1063/1.4895980]

I. INTRODUCTION

Functionality of magnetorheological elastomers (MRE) as well as magnetorheological suspensions (MRS) is due to their strong shape and rheological responses to applied magnetic fields. Understanding of these effects is the task for the theory, which by that provides fundamentals for the design and engineering of the devices comprising MREs and MRSs as essential working elements; the examples are numerous.

In the present work, we look closely at the driving mechanisms of the field-induced spatial rearrangements of the particles in MREs. The focus hereby is placed on the particles of micron size, which are the customary fillers for these materials The most popular substance for the micrograins is carbonyl iron that entails their magnetic softness and, thus, multi-domainness in the absence of external field. In this state, the net particle magnetic moments are virtual zeroes, so that their magnetic interaction is negligible. Hence, such an MRE does not differ mechanically from any other composite with a non-magnetic solid filler of the same dispersity.

When a field is imposed, the micrograins polarize becoming the sources of additional magnetic fields. As a result, each particle is engaged in magnetic (ponderomotive) interaction with the external field and with the fields of all the other grains in the sample. The particle multi-domainness ensures that the magnetization curve of such a sample is non-hysteretic and turns to zero in the absence of the external field $\boldsymbol{H}_0$. Therefore, the particle magnetic moment is of purely induced origin and can be presented as $\boldsymbol{m} = \chi_e V(\boldsymbol{H}_0 + \boldsymbol{H}_L)$, where χ_e is the external susceptibility of the particle, V its volume, and $\boldsymbol{H}_L$ the local field generated by all the other particles at the position of the given one.

If the system is dilute, i.e., on the average the particles are separated by the distances l, which are much greater than the reference grain radius a, the interparticle interactions could be treated as if each particle is a point dipole with the moment $\boldsymbol{m}$. The latter interacts with the external field via Zeeman energy $-\frac{1}{2}\mu_0(\boldsymbol{m}\boldsymbol{H}_0)$ and is coupled to all the others by the long-range dipolar potential

$$U_d = \mu_0 \sum_j^{N-1} \left[\frac{\boldsymbol{m}\cdot\boldsymbol{m}_j}{l_j^3} - \frac{3(\boldsymbol{m}\cdot\boldsymbol{l}_j)(\boldsymbol{m}_j\cdot\boldsymbol{l}_j)}{l_j^5} \right], \qquad (1)$$

where μ_0 is the magnetic permeability of vacuum, $\boldsymbol{l}_j$ is the center-to-center vector and N the total number of particles in the sample.

In MRE and MRS systems, which are attractive from practical viewpoint, i.e., those whose deformational and rheological properties are considerably changed under the field, the situation is different. As the filler density is rather high: 10–25 vol. %,[1,2] the typical interparticle distances are in the range $l \sim 2a$. Under these conditions, the dipole approximation (1) fails by definition since the particles by no means might be considered as points. Instead, one should treat them as 3D objects, whose short-range interaction is determined by the mutually induced intrinsic non-uniformities of magnetization.

This interaction is of paramount interest since it strongly affects the particle aggregation and structuring. In particular, a well-known specific feature of MREs and MRSs is that, having been subjected to a field, the particles self-organize along its direction forming long prolate aggregates (columns), whose thickness is much greater than the size of a single particle. This morphology is fully inherent to MRSs[3,4] and (with the positional restrictions imposed by the matrix) to soft MREs.[5–7]

The column morphology strikingly differs from the field-induced patterns in the assemblies of magnetically hard (single-domain) particles, i.e., those possessing permanent magnetic moments. For those systems, the dipole potential (1) is indeed a realistic one. It ensures that in a pair of

[a]Electronic mail: kam@icmm.ru
[b]Electronic mail: oleg100@gmail.com. Also at Perm National Research Polytechnic University, Perm 614990, Russia.
[c]Electronic mail: raikher@icmm.ru. Also at Mathematical Physics Department, Ural Federal University, Ekaterinburg 620083, Russia.

particles, whose magnetic moments are aligned by the external field, the configuration "head-to-tail" ($\boldsymbol{l} \parallel \boldsymbol{H}_0$) means attraction, while the "side-by-side" ($\boldsymbol{l} \perp \boldsymbol{H}_0$) pattern corresponds to repulsion. This "lateral" repulsion spans over the angle interval defined by condition $\cos^2\gamma \leq 1/3$, where γ is the angle between $\boldsymbol{l}$ and $\boldsymbol{H}_0$. A direct result of the dipole interaction (1) of the magnetic moments is that the field-induced aggregation starts with formation of short chains, which have only one particle in their cross-section.

As there is a direct analogy between electrically and magnetically polarizable particle assemblies—it requires just to replace the magnetic fields by the electric ones—a lot of knowledge on the particle field-induced interaction and aggregation can be taken from the well-developed theory of electrorheological fluids. In particular, this concerns column formation in dense systems and the inner structure of the columns that is proven to resemble the so-called body-centered tetragonal (bct) lattice.[8–10]

Self-organization of the particles in MREs undergoes in a more complex way than in MRSs, because the aggregation process is strongly impeded by the elastic forces developing in the polymer matrix in response to the particle displacements. Evidently, this magneto-elastic interplay is an exclusive feature of MREs. Hereby, we consider the simplest problem of this type, namely, the behavior of a pair of magnetically polarizable particles in a polymeric matrix. One of the particular objectives of this consideration is to shade light on the mechanism of the so-called magnetic shape memory effect. Namely, the sufficiently dense MREs are known to be able, when magnetized, to change drastically their rheology from elastic-like to plastic-like one.[6,11] As long as the field is on, the MRE, like a putty, easily deforms without inducing any restoring forces. Upon turning off the field, the magnetic forces zero out, and the sample restores its initial shape. The only existing qualitative explanation for the effect employs the hypothesis of "magnetic staples,"[12,13] i.e., small tight particle clusters. It helps in phenomenological modeling but is unable to clarify the mesoscopic mechanism of the effect.

In Sec. II, the problem of magnetic interaction of the particles at close distances is reviewed and an interpolation formula for the "multipolar" potential is proposed. In Sec. III, the elastic energy arising in the matrix due the particle mutual approach is considered, a pertinent approximate expression for it is derived and justified. Minimization of the combined magnetoelastic energy of the particle pair is done and analyzed in Sec. IV. We show that in a certain field range this system is bistable, i.e., displays hysteretic behavior under the change of the applied field. One of the equilibrium states of the pair corresponds to a weakly deformed configuration, while the other is cluster-like, thus resembling an elementary "magnetic staple." The macroscopic consequences of the found mesoscopic magnetoelastic hysteresis are discussed in Sec. V and then summarized in Sec. VI.

II. INTERACTION OF POLARIZABLE PARTICLES

Each polarizable particle, when subjected to an external field, becomes the source of polarization for its neighbors, and as well, polarizes in response to their fields. Such a particle should be treated as a finite object whose magnetic state, instead of a single vector $\boldsymbol{m}$, is determined by a non-uniform spatial distribution of magnetization $\boldsymbol{M}(\boldsymbol{r})$ inside the particle. In this aspect, the problem is very much alike those addressed in micromagnetism.[14] The form of $\boldsymbol{M}(\boldsymbol{r})$ plays the decisive role in the short-range particle coupling. Note that this interaction, unlike the point-dipole one, it is not additive: the energy of, e.g., three particles at close distances cannot be presented as a sum of three respective pair potentials.[15]

The problem of the field-induced interaction of a pair of spherical polarizable particles is a classical one. In here we restrict ourselves by the case of linear polarizability that implies either those particles made of a (super)paramagnetic material or the multi-domain ferromagnetic ones provided the field is sufficiently low, and the magnetization curve of the material is yet quasi-linear. The exact solution (in the form of infinite series) of the pertinent Laplace equation had been first published about a century ago.[16] Being of general interest, it repeatedly turns up in diverse contexts: hydrodynamic,[17] elastic,[18] thermophysical,[19] electro-,[10,20–22] and magnetorheological.[23,24] The two conventional representations of the said solution differ by the choice of the coordinates: either a single bispherical[16] or a pair of spherical frames.[19–22,24] Either of them yields the magnetic interparticle energy in the general form

$$U_{mp}(q,\gamma) = \omega_0(q) + \omega_2(q)\cos^2\gamma. \tag{2}$$

Functions ω_α are presented in the form of multipole expansions, i.e., the series in inverse powers of parameter $q = l/a$. This analytical procedure is rather cumbersome, and the labor to evaluate the series coefficients grows drastically with the increase of the length of the series, see, for example, Ref. 19, where they are given up to q^{-9}. Meanwhile, the number of terms needed to accurately find U_{mp} for the case of close particle contact ($q \to 2$), amounts to hundreds. As well, this number grows with the magnetic permeability mismatch $\alpha = \mu_p/\mu$, where μ_p and μ are the permeabilities of the particle material and the embedding matrix, respectively.

Since evaluation of U_{mp} by exclusively analytical treatment is not feasible, the expansion coefficients should be found numerically. In Ref. 22, this was done numerically to q^{-25}, which worked up to $q = 2.02$ and for α as large as 5. This range fits well the case of electrorheological suspensions (μ is replaced by dielectric permeability ε) but does not suffice for the magnetic case since parameter α for iron against water or a polymeric solution amounts to many hundreds. Besides, when studying structure transformations in MRE(S)s, one needs to know interparticle forces, not energies. This implies differentiating of expression (2) with respect to l, and, thus, involves one more numerical procedure that efficiently spoils accuracy. To retain it in final results, one has to substantially precise the data on U_{mp}.

Searching the way to facilitate the work, we, first, have built up a program to evaluate U_{mp} from the exact solution (multipole expansion) truncating it at an arbitrary order in $1/q$. By taking the increasing number of terms, we have found that a series of about 100 multipoles suffices to describe the interparticle

forces with high accuracy ($\sim 10^{-2}\%$) whatever q (up to full surface contact) and γ, and the permeability mismatch α ranging from 10^2 to 10^4 (aiming at iron microparticles).

Then, using these numeric results as a benchmark, interpolation formulas were constructed, which ensure accuracy better than 1% inside the interval of interparticle distances, where the short-range (multipole) forces differ significantly from the dipole approximation. The obtained expression is as follows:

$$U_{mp}(q,\gamma) = -3\mu_0\mu H_0^2 V \sum_{k=3}^{7} \left(\frac{\alpha-1}{\alpha+2}\right)^{p_k} \times \left[\frac{a_k}{(q-b_k)^k} + \frac{c_k}{(q-d_k)^k}\cos^2\gamma\right]. \quad (3)$$

The coefficients in formula (3) are given in Table I.

From formula (3), the interparticle force is obtained in a standard way as

$$\boldsymbol{f} = \boldsymbol{f}_n + \boldsymbol{f}_\tau, \quad \boldsymbol{f}_n = -\frac{\boldsymbol{q}}{a}\left(\boldsymbol{q}\cdot\frac{\partial U_{mp}}{\partial \boldsymbol{q}}\right), \quad \boldsymbol{f}_\tau = \frac{1}{a}\left(\boldsymbol{q}\times\left(\boldsymbol{q}\times\frac{\partial U_{mp}}{\partial \boldsymbol{q}}\right)\right), \quad (4)$$

where $\boldsymbol{q} = \boldsymbol{l}/a$. As seen, $\boldsymbol{f}_n$ is the component along the center-to-center vector, while $\boldsymbol{f}_\tau$ is perpendicular to $\boldsymbol{f}_n$ and lies in the plane made by vectors $\boldsymbol{q}$ and $\boldsymbol{H}_0$. The force couple $\boldsymbol{f}_\tau$ produces the torque

$$\boldsymbol{M} = a(\boldsymbol{q}\times\boldsymbol{f}_\tau) = -a\left(\boldsymbol{q}\times\frac{\partial U_{mp}}{\partial \boldsymbol{q}}\right), \quad M = -\frac{\partial U_{mp}}{\partial \gamma}. \quad (5)$$

The difference between the point-dipole and multipole results is illustrated in Fig. 1 for the cases of the center-to-center force $\boldsymbol{f}_n$ in the "head-to-tail" ($\gamma = 0$) and "side-by-side" ($\gamma = 90^\circ$) configurations.

The data shown in Fig. 1(a) infer that the particle pairs (dimers) in MREs and MRSs, once formed in the direction of the field, are much stronger those of point dipoles. On the other hand, the lateral ($\gamma = 90^\circ$) repulsion force, see Fig. 1(b), is notably weaker. The qualitative difference between those two types of interaction becomes clear when comparing the angle dependencies $\boldsymbol{f}_n$. The geometry scheme and the function plots are presented in Fig. 2.

Setting the coordinate origin at the center of particle 1, from Fig. 2(a) one sees that according to the point dipole model particle 2 is attracted if its center is inside the region $\gamma < \gamma_0$ and is repelled otherwise, i.e., at $\gamma > \gamma_0$. The straight

TABLE I. Numerical coefficients for the interpolation formula (3).

k	a_k	b_k	c_k	d_k	p_k
3	−1	0	3	0	2
4	0	0	3.42×10^{-2}	1.3976	3
5	0.111	−0.689	2.83×10^{-6}	1.8947	11
6	0.509	0.589	1.8×10^{-13}	1.9898	13
7	−0.424	0.592	0	0	20

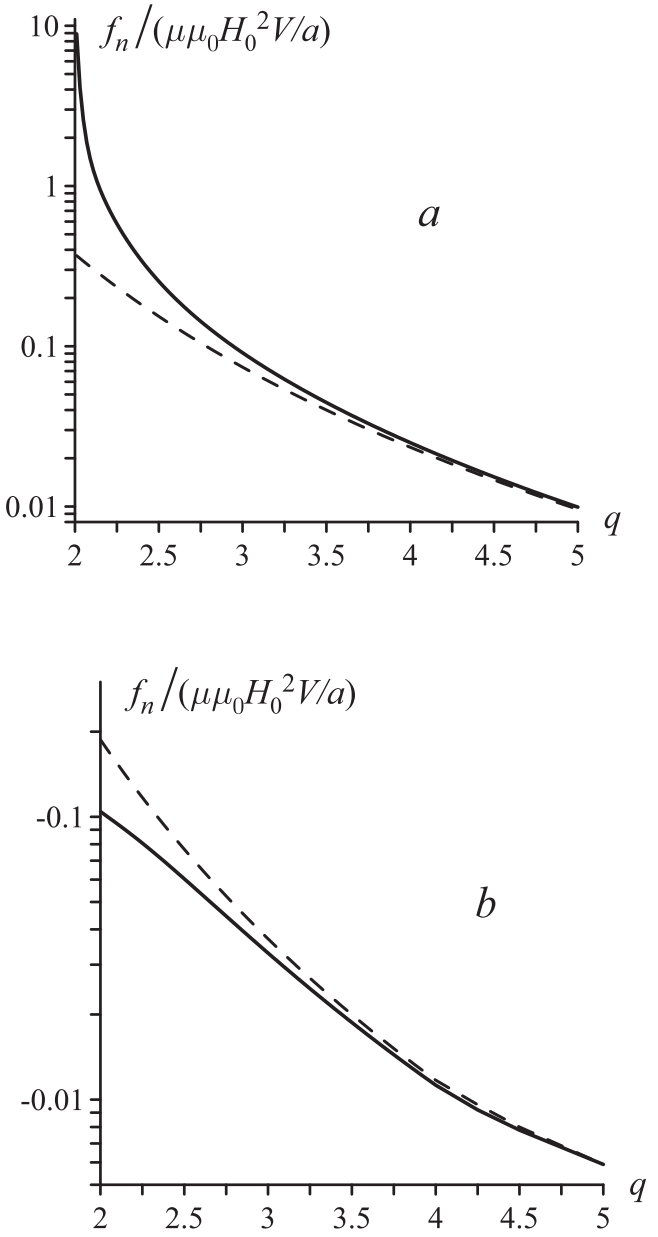

FIG. 1. Center-to-center force in a pair of polarizable particles with $\alpha = 10^3$ in $\gamma = 0$ (*a*) and $\gamma = 90^\circ$ (*b*) configurations; point-dipole approximation (dashed), multipole calculation with about 100 terms (solid); positive sign corresponds to attraction and negative to repulsion forces; note the logarithmic scale of the vertical axis.

dashed lines in Figs. 2(a) and 2(b) correspond to $\gamma_0 = 54.7^\circ$ and, thus, to the "neutrality" condition $\boldsymbol{f}_n = 0$. Such a distribution of interparticle forces implies that a monodisperse assembly of point-dipole particles, being subjected to a field, begin to self-arrange as one-particle thick strands.

The situation for the magnetizable particles is different, as is shown by the solid lines in Fig. 2. In this case, the sign of interaction force $\boldsymbol{f}_n$ depends on the interparticle distance. In close vicinity of particle 1, particle 2 is attracted at almost any angle except for the narrow interval $84.3^\circ < \gamma < 90^\circ$. We note that Fig. 2 details the force distribution only in the $0 < \gamma < 90^\circ$ quadrant, but the solutions described possess azimuthal as well as inversion ($\boldsymbol{H}_0 \to -\boldsymbol{H}_0$) symmetry.

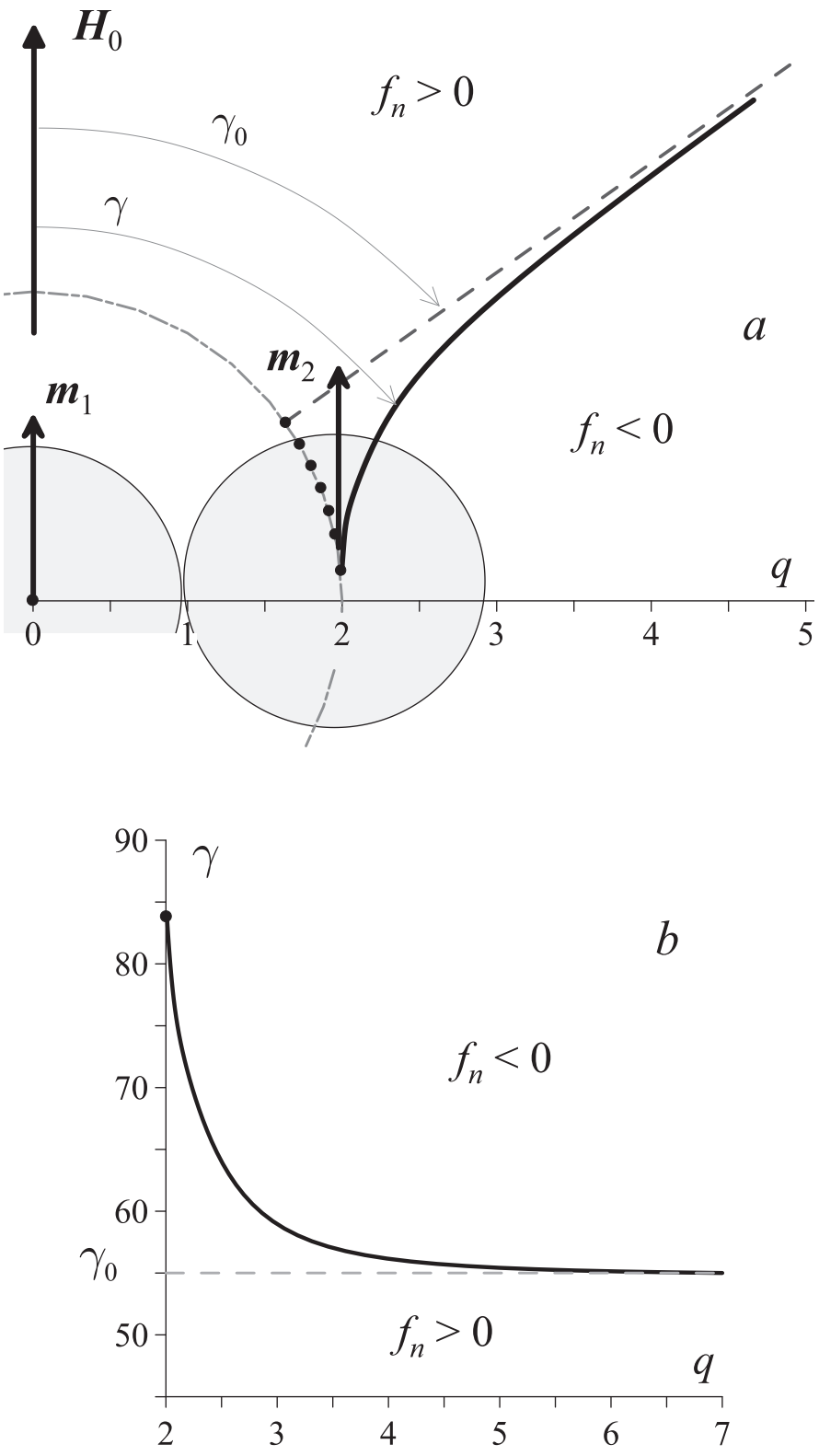

FIG. 2. Regions of mutual attraction/repulsion separated by "neutral" lines ($f_n = 0$). In the polar plot (a) straight dashes show neutral line for point dipoles, solid curve is the same for magnetizable particles; the dots mark possible positions of the center of magnetizable particle 2, where it is attracted at $q = 2$; in plot (b) the "neutral" angle for point dipoles is constant: $\gamma_0 = 54.7°$, for magnetizable particles it grows up to $\gamma = 83.4°$ at the particle contact.

III. ELASTIC ENERGY OF THE PARTICLE PAIR

In MRSs, where the particles are virtually free, the magnetic interaction is the sole cause of aggregation. In MREs, where the particles in the no-strain/field-off state keep certain equilibrium positions in the polymer matrix, the action of magnetic forces in the field-on state is counteracted by elasticity. Due to that the rearrangement of the particles inside a magnetized MRE results from minimization of the sum of magnetic and elastic energies. In this section, we work out an approximation for the latter.

Note that if the elasticity is linear (Hookean) then the deformation field around the particles obeys the same Laplace equation as that describing their magnetic potential, and, thus, an exact solution is available.[18] However, in the case of MREs, the Hook model is practically useless,

since—see Ref. 25, for example—for elastomers, it works quite poorly even at small strains. The more so it is for the interparticle distances $l \sim 2a$, where the local strains are indeed high.

To construct an analytical approximation compatible with the elastomer rheology, we take the Mooney-Rivlin (hyperelastic) model, where the potential (energy volume density) is

$$W = c_1\Big\{\big[J^{-2/3}I_1(\mathbf{C}) - 3\big] + \tilde{c}_2\big[J^{-4/3}I_2(\mathbf{C}) - 3\big] + \frac{1}{2}\tilde{K}(J-1)^2\Big\}. \tag{6}$$

Here I_1, I_2, I_3 are the invariants of the Cauchy-Green tensor $\mathbf{C}$ related to the Green-Lagrange deformation tensor $\mathbf{E}$ as $\mathbf{C} = 2\mathbf{E} + \mathbf{I}$, where $\mathbf{I}$ is unit tensor and $J = \sqrt{I_3(\mathbf{C})}$ the Jacobian. Keeping c_1 a free parameter (for small deformations $2c_1(1+\tilde{c}_2)$ is the shear modulus), the other constants of expression (6) we set $\tilde{c}_2 = 0.1$ and $\tilde{K} = 10^3$ thus assuming that the elastomer is weakly compressible. As potential W is nonlinear, the pertinent Laplace equation cannot be solved exactly. A standard way to solve it for a Mooney-Rivlin material is via finite-element method. This, however, does not yield analytical forms and, thus, is not fit for further minimization. Instead, we construct a formula with a few parameters capable to reproduce the numerical (i.e., virtually exact) results for a Mooney-Rivlin elastomer. This is done with the aid of a heuristic scheme shown in Fig. 3.

In Fig. 3, two particles are separated by the equilibrium distance l_0, and to each particle two solid plates are attached, one of which is step-shaped. In between, three elastic cylindrical rods are set along Oz axis. The shortest rod (1) has radius r_1 and length $l_1 = h_0 = l_0 - 2a$; the two other rods with radii r_2 and lengths $l_2 = h_0 + a$ are positioned alongside and parallel to it. The solid plates ensure uniform strain of rods 1 and 2 when the particles move along Oz. The "external" rods (3) have lengths $l_3 = h_0$ and radii r_3; their outer ends abut on unmovable walls, where the normal (but not tangential) displacements are forbidden.

Reliability of the proposed scheme has been proven by comparison with numerical simulations of the stress-strain behavior of a Mooney-Rivlin matrix containing two solid spherical inclusions. For that, we use SfePy (Simple finite element in Python) package.[26] The model sample is a cube with the edge d, inside which two spherical "holes" are positioned

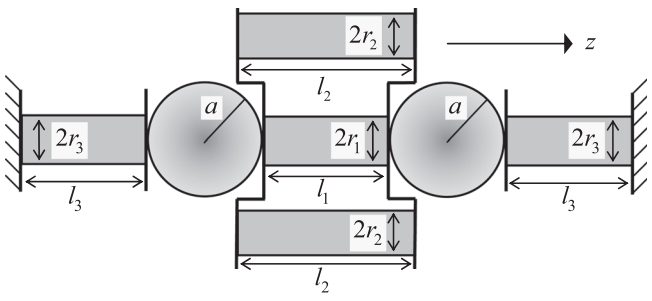

FIG. 3. Elastic element scheme imitating stress-strain behavior of a pair of particles under axial displacement.

along the line (Oz axis) connecting the centers of opposing faces of the cube. The variational problem takes the form

$$\int_{\Omega_0}[\mathbf{S}_{\text{eff}}(u) + \tilde{K}(J-1)J\mathbf{C}^{-1}]\cdot\cdot\,\delta\mathbf{E}dV = 0, \tag{7}$$

where Ω_0 is the initial configuration of the sample. Imposing symmetry requirements $x \leftrightarrow -x$ and $y \leftrightarrow -y$, the problem (7) is solved for a quarter of the cube under the following boundary conditions for the displacements:

$$\boldsymbol{u}|_{\Gamma_1} = \boldsymbol{u}_1 = (0,0,-u), \quad \boldsymbol{u}|_{\Gamma_2} = \boldsymbol{u}_2 = (0,0,u),$$
$$\boldsymbol{u}_x|_{x=0} = 0, \quad \boldsymbol{u}_y|_{y=0} = 0, \tag{8}$$

here $\Gamma_{1,2}$ are the surfaces of the particles 1 and 2, respectively; the effective stress tensor is evaluated as

$$\mathbf{S}_{\text{eff}}(\boldsymbol{u}) = 2J^{-2/3}\left[I - \frac{1}{3}I_1(\mathbf{C})\mathbf{C}^{-1}\right] + 2\tilde{c}_2J^{-4/3}\left[I_1(\mathbf{C})\,\mathbf{I} - \mathbf{C} - \frac{2}{3}I_2(\mathbf{C})\mathbf{C}^{-1}\right].$$

As seen from Eq. (8), the mutual approach of the "holes" is imposed by vectors $\boldsymbol{u}_1$ and $\boldsymbol{u}_2$, which render a given displacement u to all the points of the surfaces of both "holes". Due to that, the action of such "holes" on the surrounding matrix is equivalent to that of solid particles of the same radius a. The displacement is enhanced discretely from zero (initial state) up to the maximum corresponding to the nearly tight contact of the particles. At each step in u, the elastic problem is solved, and the displacement field in the sample is obtained. From it, first, the Cauchy-Green deformation and then the potential W are found. Finally, the elastic energy of the sample $U_{el} = \int W dV$ as a function of $q = l/a$ is evaluated. Each series of calculations begins with setting the non-dimensional value for the initial interparticle distance $q_0 = l_0/a$ and the non-dimensional size $d = 4(q_0 + 2)$ of the cube.

The finite-element mesh is thickened around the holes complying with the non-uniformity of the stress-strain distributions. Doing that with regard to the available computational resources, we choose the reference size of the mesh cell as 0.05 a near the hole surface and 0.4 a at the outer boundary of the sample cube. Using these parameters, data arrays $U_{el}(q, q_0)$ had been obtained with supercomputer SL390s/SL270s Uran.[27]

The numerical representation of the elastic energy $U_{el}(q, q_0)$ enables one to evaluate the parameters of the scheme of Fig. 3. Upon mutual approach of the "holes," rods 1 and 2 shrink, while rods 3 elongate. The arising strains are in a simple way expressed in terms of displacement u:

$$\lambda_1 = \frac{l_1 - 2u}{l_1} = \frac{h_0 - 2u}{h_0}, \quad \lambda_2 = \frac{l_2 - 2u}{l_2} = \frac{h_0 + 1 - 2u}{h_0 + 1}, \quad \lambda_3 = \frac{l_3 + u}{l_3} = \frac{h_0 + u}{h_0}. \tag{9}$$

Deriving the Gauchy-Green tensor for each λ_n in Eq. (9), one arrives at the elastic potential of a rod made of the Mooney-Rivlin material:

$$W = c_1\{[I_1(\mathbf{C}_n) - 3] + \tilde{c}_2[I_2(\mathbf{C}_n) - 3]\},$$

where the invariants are $I_1(\mathbf{C}_n) = 2/\lambda_n + \lambda_n^2$ and $I_2(\mathbf{C}_n) = 2/\lambda_n^2 + 2\lambda_n$ with $n = 1,\ 2,\ 3$. Since the rod volume is $V_n = \pi r_n^2 l_n$, the elastic energy of the whole scheme takes the form

$$U_{el} = \pi r_1^2 l_1 W(\lambda_1) + 2\pi r_2^2 l_2 W(\lambda_2) + 2\pi r_3^2 l_3 W(\lambda_3). \quad (10)$$

In formula (10), the approximation parameters are radii r_{1-3}; their values for several initial interparticle distances are given in Table II.

As tested, this approximation reproduces all the data on U_{el} with accuracy not worse than 0.1% for the interparticle distances $q \geq 2.5$. Assuming its reliability at smaller q as well, we use Eq. (10) to evaluate the elastic energy down to $q \sim 2$, where the computer simulation is unstable.

IV. BISTABILITY EFFECT

The reference particle size in MREs ranges from several microns to several tens of microns. The thermal motion of such particles is rather weak. Given that equilibrium configurations of the pair of magnetizable particles embedded in an elastomer might be found from minimization of the sum of the magnetic (3) and elastic (10) energies. Consider the "head-to-tail" configuration of the pair. The non-dimensional form of the total energy is

$$\tilde{U} = (U_{mp} + U_{el})/(c_1 a^3) = \tilde{H}_0^2[\omega_0(q) + \omega_2(q)] + \pi[r_1^2 l_1 \tilde{W}(\lambda_1) + 2r_2^2 l_2 \tilde{W}(\lambda_2) + 2r_3^2 l_3 \tilde{W}(\lambda_3)], \quad (11)$$

where $\tilde{W} = W/c_1 = I_1(\mathbf{C}_n) - 3 + \tilde{c}_2[I_2(\mathbf{C}_n) - 3]$ and parameter $\tilde{H}_0 = H_0/\sqrt{c_1}$ is introduced.

The behavior of potential $\tilde{U}(q, q_0, \tilde{H}_0)$, whose minima determine the equilibrium interparticle distance under a given field, is shown in Fig. 4. When the field is weak, so is the induced strain. To roughly ascertain the particle displacement in this case, we set elasticity to be Hookean. At high magnetic permeability of a ferromagnet, the calculation similar to that outlined in Ref. 28 yields $q = q_0[1 - 96\pi^2\mu_0\tilde{H}_0^2/q_0^6]$, thus indicating that the system has a single energy minimum corresponding to small mutual approach of the particles. In Fig. 4(a), this situation is reflected by curve 1.

Upon the field increase, the magnetic interparticle forces grow along with the particle magnetization. This entails a qualitative change of the situation. Besides the state of weak compression, there emerges another energy minimum corresponding to close approach of the particles and, thus, strong deformation of the matrix, see curve 2 in Fig. 4(a). This means that the system becomes bistable and can attain either

TABLE II. Numerical coefficients for the interpolation formula (10).

q_0	r_1/a	r_2/a	r_3/a
2.5	1.3×10^{-2}	0.76	0
3	2.3×10^{-2}	0.60	0.61
3.5	2.6×10^{-2}	0.49	0.97
4	2.5×10^{-2}	0.43	1.21

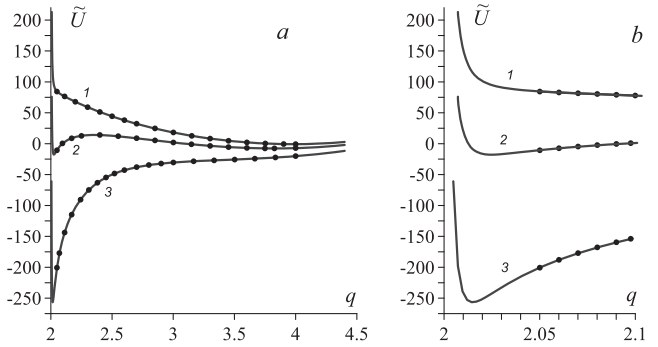

FIG. 4. Magnetoelastic energy of a pair under change of the applied field strength (a) in general and (b) in the vicinity of $q = 2$; initial interparticle distance is $q_0 = 4$, the field strength is $\tilde{H}_0 = 5$ (1), 15 (2), and 25 (3); dots mark the values of $\tilde{U}$ obtained from the finite element solution.

of the two equilibrium states. On further increase of $\tilde{H}_0$, the weak-deformation minimum disappears, and the collapsed (dimer) state remains the only possible one, see curve 3. As soon as the dimer is formed, the equilibrium interparticle distance becomes virtually independent of the field strength. This is clearly visible in Fig. 4(b), which expands the part of Fig. 4(a) in the vicinity of $q = 2$. This reflects a well-known fact that a real elastomer, when strongly stressed, is very stiff.

We remark that the use of approximation (11) in the region $q \sim 2$, where the numerical solution is not available, entails some uncertainty in evaluation of the position q_{min} of the cluster-type minimum. However, in qualitative aspect, the results presented in Fig. 5 are completely justified. Moreover, as the second minimum always means close neighboring of the particles, the differences between exact and approximate values of q_{min} are not very important.

The above-described bistability effect implies that the transitions between the equilibrium configurations of the pair occur in a hysteretic manner. Let us assume that the particle pair responds to turning on a weak field ($\tilde{H}_0 \ll 1$) by

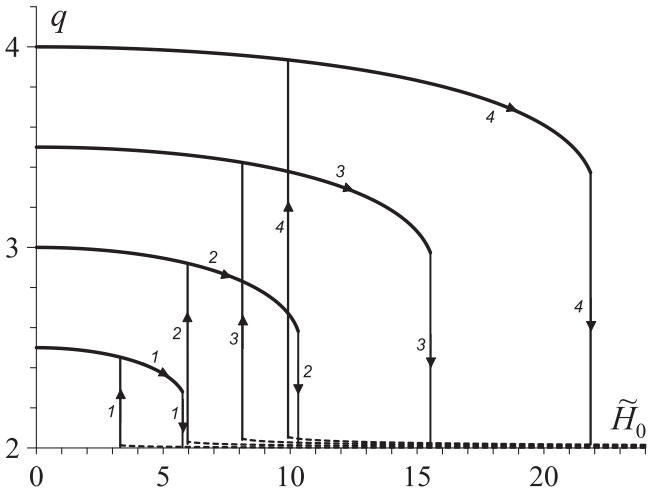

FIG. 5. Equilibrium interparticle distance in the "head-to-tail" configuration of the particles in a field cycle; particle initial separations are $q_0 = 2.5$ (1), 3 (2), 3.5 (3), and 4 (4), arrows mark the directions of the displacements; dotted lines show the branches obtained with the aid of extrapolation; the elastic constant $\tilde{c}_2 = 0.1$.

deformation $l_0 - l \ll l_0$. Upon increase of the field, the system would reside in this particular state even after appearance of the second minimum because thermal fluctuations are negligible. The weakly deformed configuration would cease to exist only when the "distant" minimum of the energy would disappear, cf. curves 2 and 3 in Fig. 4. As a result, the particles would move into the only remained "close" minimum thus forming a dimer. In the inverse process (diminution of the field), the same scenario applies to the restoration of the initial configuration of the pair.

Displacement hysteresis loops of the particle pair under a cyclic change of the field are presented in Fig. 5. In each loop, the vertical lines mark the lower and upper bounds of the bistability region with respect to $\tilde{H}_0$. The branches of functions $q(\tilde{H}_0)$ adjacent to the $\tilde{H}_0$ axis are given by dotted lines since they are plotted with the aid of approximation formula (11).

V. DISCUSSION

We remark on drastic distinction between the magnetostatics forces in a pair of point-dipole and in a pair of magnetizable particles. This is essential for sufficiently dense MRE(S)s where the point-dipole model is inappropriate. The wide region of attraction around a magnetizable particle infers that, when subjected to a field, the particles are strongly inclined not only to form single-particle chains along the field but also to unite with those particles located in their lateral vicinity. This supports visual observations that particle aggregation in MRSs nucleates via formation of "droplets" rather than the strands, which are one-particle wide.

The bistability effect in a pair of magnetizable particles embedded in an elastic matrix is of apparent importance for MREs. It favors abundant clusterizing accompanied by shrinking of the sample in the direction of the field and a substantial change of rheology of the material. Both these phenomena turn up in experiments. However, compression, often predicted as well on the basis of the point-dipole model,[29–33] is observed quite rarely.[34] Most probably, this is due to the chaotic nature of MREs prepared in the absence of external field. Indeed, along with the pairs approximately parallel to the direction of the imposed field, there is a number of particles, which are already pre-clusterized. MREs inherit them from the magnetic powder due to imperfect technique of dispersing. If a pre-existing cluster is even slightly anisometric, when magnetized, it strives to align its longest axis along the applied field. Such a rearrangement induces elongation of the sample both locally and macroscopically.[31] As in a real sample all kinds of particle configurations are present, then, depending on the details of the particle short-range spatial order, one might encounter elongation as well as compression or virtual absence of the magnetic striction.

Another consequence of the internal clusterization is insensitive to the sign of the macroscopic magnetic striction. Dense MREs are known to change drastically their rheology from elasticity to plasticity.[6,11] The hypothesis of "magnetic staples"[12,13] invented to explain the effect assumes that the particles form a set of clusters. This structure responds to mechanical load by relocation of particles between the clusters. This inter-cluster particle exchange has low thresholds, so that the magnetic energy of the sample remains at approximately the same level. Due to that the sample readily deforms under low loads without displaying any significant resistance forces. Note, however, that in this process, the polymer molecules attached to the particles surfaces, unwound but do not break. As soon as the field is switched off, the particles lose their magnetization. Then the relatively weak elastic forces, formerly completely dominated by the magnetic ones, restore the initial shape of the sample. Therefore, the hysteretic displacements of magnetizable particles embedded in a polymer seem to provide a reasonable explanation for the occurrence of magnetic plasticity in MREs.

Here, we demonstrated it for pair clusters, but it is reasonable to surmise that it makes the base of the collective effect of the same origin as well. Certainly, to get a description for the net observable plastic behavior effect one needs to allow for the polydispersity of the particles, the presence of pre-existing clusters, etc. Moreover, one has to take into account that the field-induced deformation of the sample is governed by at least two mechanisms: the short-range and long-range (shape effect) ones, which might work coherently or counteract.[31,33]

VI. CONCLUSIONS

Combination of magnetic and elastic interactions in a pair of magnetizable particles embedded in an elastic matrix is considered. In the magnetic aspect, the difference of the situation from that of point dipoles is that in the vicinity of a magnetizable particle attraction completely dominates repulsion. A robust interpolation formula to describe this interaction and to facilitate calculation of the interparticle forces is proposed.

An interpolation expression for the elastic interaction of the particles under their mutual approach is constructed with the aid of a heuristic rheological scheme. The reliability of this formula is tested against the numerical solution of the same problem. Combining these two interpolations, the magnetoelastic energy of a pair of particles subjected to an external field is obtained for the "head-to-tail" configuration. Analysis shows that, depending on the field strength, the pair might dwell in a state of weak compression or collapse forming a cluster. In a certain range of field strength the system is bistable and might assume any of these states. As the thermal motion has virtually no effect on the particle behavior, the transitions between the weakly compressed and cluster configurations should occur in a hysteretic manner. The signatures of such a behavior could be found in the reported experimental data.

The above-described bistability effect provides a mesoscopic justification for the phenomenological model of "magnetic staples," which explains the field-induced plasticity observed in dense MREs.

An important limitation of the built-up description is the assumption of linear polarizability of the particle material.

Meanwhile, MREs are intended to work in the fields, which can easily saturate the particles. In this case—it never occurs in electrorheology—the above-used series expansions are not valid and should be replaced by a numerical model. As the next step, a finite-element treatment of the magnetic interaction problem is being developed in order to overcome the limitations imposed by the requirement of linear magnetization.

ACKNOWLEDGMENTS

The work was supported by RFBR Grant Nos. 14-02-96003 and 13-01-96056, UB RAS Program No. 10 (12-P-1018) and project MIG S26/617 from the Ministry of Education and Science of Perm Region.

[1]Y. Wang, Y. Hu, X. Gong, W. Jiang, P. Zhang, and Z. Chen, "Preparation and properties of magnetorheological elastomers based on silicon rubber/polystyrene blend matrix," J. Appl. Polym. Sci. **103**, 3143–3149 (2007).
[2]H. Böse, "Viscoelastic properties of silicone-based magnetorheological elastomers," Int. J. Mod. Phys. B **21**, 4790–4796 (2007).
[3]B. J. Park, F. F. Fang, and H. J. Choi, "Magnetorheology: Materials and application," Soft Matter **6**, 5246–5253 (2010).
[4]J. De Vicente, D. J. Klingenberg, and R. Hidalgo-Alvarez, "Magnetorheological fluids: A review," Soft Matter **7**, 3701–3710 (2011).
[5]L. V. Nikitin, L. S. Mironova, A. N. Samus, and G. V. Stepanov, "The influence of a magnetic field on the elastic and viscous properties of magnetoelastics," Polymer Sci. Ser. A **43**, 443–450 (2001).
[6]G. V. Stepanov, D. Yu. Borin, Yu. L. Raikher, P. V. Melenev, and N. S. Perov, "Motion of ferroparticles inside the polymeric matrix in magnetoactive elastomers," J. Phys.: Condens. Matter **20**, 204121–5 (2008).
[7]D. Günther, D. Borin, S. Günther, and S. Odenbach, "X-ray microtomographic characterization of field-structured magnetorheological elastomers," Smart Mater. Struct. **21**, 015005–7 (2012).
[8]R. Tao and J. M. Sun, "Ground state of electrorheological fluids from monte carlo simulations," Phys. Rev. A **44**, R6181–R6184 (1991).
[9]R. Tao and Q. Jiang, "Simulation of structure formation in an electrorheological fluid," Phys. Rev. Lett. **73**, 205–208 (1994).
[10]R. Tao, Q. Jiang, and H. K. Sim, "Finite-element analysis of electrostatic interactions in electrorheological fluids," Phys. Rev. E **52**, 2727–2735 (1995).
[11]L. V. Nikitin, G. V. Stepanov, L. S. Mironova, and A. I. Gorbunov, "Magnetodeformational effect and effect of shape memory in magnetoelastics," J. Magn. Magn. Mater. **272–276**, 2072–2073 (2004).
[12]P. V. Melenev, Yu. L. Raikher, V. V. Rusakov, and G. V. Stepanov, "Field-induced plasticity of soft magnetic elastomers," J. Phys.: Conf. Ser. **149**, 012094–5 (2009).
[13]P. V. Melenev, Yu. L. Raikher, G. V. Stepanov, V. V. Rusakov, and L. S. Polygalova, "Modeling of the field-induced plasticity of soft magnetic elastomers," J. Intell. Mater. Syst. Struct. **22**, 531–538 (2011).
[14]W. F. Brown, *Micromagnetics* (Interscience Publishers, 1963).
[15]H. J. H. Clerx and G. Bossis, "Many body electrostatic interactions in electrorheological fluids," Phys. Rev. E **48**, 2721–2729 (1993).
[16]G. B. Jeffery, "On a form of the solution of Laplace's equation suitable for problems relating to two spheres," Proc. Roy. Soc. (London) Ser. A **87**, 109–120 (1912).
[17]J. Happel and H. Brenner, *Low Reynolds Number Hydrodynamics* (Prentice-Hall, Englewood Cliffs, NJ, 1965).
[18]J. F. Shelly and Y.-Y. Yu, "The effect of two rigid spherical inclusions on the stresses in an infinite elastic solid," Trans. ASME **33**, 68–74 (1966).
[19]D. J. Jeffrey, "Conduction through a random suspension of spheres," Proc. Roy. Soc. (London) Ser. A **335**, 355–367 (1973).
[20]D. K. Ross, "The potential due to two point charges each at the centre of a spherical cavity and embedded in a dielectric medium," Aust. J. Phys. **21**, 817–822 (1968).
[21]D. J. Klingenberg and C. F. Zukoski, "Studies of the steady-shear behavior of electrorheological suspensions," Langmuir **6**, 15–24 (1990).
[22]Y. Chen, A. F. Sprecher, and H. Conrad, "Electrostatic particle-particle interactions in electrorheological fluids," J. Appl. Phys. **70**, 6796–6803 (1991).
[23]L. C. Davis, "Model of magnetorheological elastomers," J. Appl. Phys. **85**, 3348–3351 (1999).
[24]E. E. Keaveny and M. R. Maxey, "Modeling the magnetic interactions between paramagnetic beads in magnetorheological fluids," J. Comput. Phys. **227**, 9554–9571 (2008).
[25]P. Oswald, *Rheophysics: The Deformation and Flow of Matter* (Cambridge University Press, 2009).
[26]See www.sfepy.org for SfePy: Simple Finite Elements in Python (2014).
[27]See s.top500.org/static/lists/2013/06/TOP500-201306.xls for Top 500 Supercomputer Sites (2013).
[28]P. V. Melenev, V. V. Rusakov, and Yu. L. Raikher, "Magnetic behavior of in-plane deformable dipole clusters," J. Magn. Magn. Mater. **300**, e187–e190 (2006).
[29]L. Borcea and O. Bruno, "On the magneto-elastic properties of elastomer ferromagnet composites," J. Mech. Phys. Solids **49**, 2877–2919 (2001).
[30]D. S. Wood and P. J. Camp, "Modeling the properties of ferrogels in uniform magnetic fields," Phys. Rev. E **83**, 011402–9 (2011).
[31]O. V. Stolbov, Yu. L. Raikher, and M. Balasoiu, "Modelling of magnetodipolar striction in soft magnetic elastomers," Soft Matter **7**, 8484–8487 (2011).
[32]J. M. Ginder, S. M. Clark, W. F. Schlotter, and M. E. Nichols, "Magnetostrictive phenomena in magnetorheological elastomers," Int. J. Mod. Phys. B **16**, 2412–2418 (2002).
[33]D. Ivaneyko, V. Toshchevikov, M. Saphiannikova, and G. Heinrich, "Mechanical properties of magneto-sensitive elastomers: Unification of the continuum-mechanics and microscopic theoretical approaches," Soft Matter **10**, 2213–2225 (2014).
[34]G. Y. Zhou and Z. Y. Jiang, "Deformation in magnetorheological elastomer and elastomerferromagnet composite driven by a magnetic field," Smart Mater. Struct. **13**, 309–316 (2004).